Frontiers in Scientific Research and Technology

Online ISSN: 2682-2970
Print ISSN: 2682-2962
http://fsrt.journals.ekb.eg

FSRT J 12 (2025) 32 - 45 10.21608/fsrt.2025.397370.1170

Piecewise Cancer Tumor Disease of Partial Differential Equations Based on Exponential and Non-Singular Kernel: Numerical Treatments

Nasser H. Sweilam[1*], Seham M. Al-Mekhlafi[2], Waleed S. Abdel Kareem[3], Ghader Alqurishi[3]

[1]Mathematics Department, Faculty of Science, Cairo University, Giza, Egypt

[2]Mathematics Department, Faculty of Education, Sana'a University, Yemen

[3]Department of Mathematics, Faculty of Science, Suez University, Suez, Egypt

ARTICLE INFO

Article history:
Received 24 June 2025
Received in revised form 3 September 2025
Accepted 3 September 2025
Available online 6 September 2025

Keywords
Cancer tumor;
Additive Gaussian ;
Ahemotherapy drugs;
Nonlinear partial differential equation;
Caputo–Fabrizio operator.

ABSTRACT

We propose a novel fractional–stochastic reaction–diffusion model for cancer dynamics that integrates the Caputo–Fabrizio derivative with additive Gaussian noise within a piecewise temporal framework. The model characterizes the nonlinear spatiotemporal interactions among normal tissue, tumor cells, immune responses, and chemotherapeutic agents. Fractional-order derivatives with exponential kernels account for memory and nonlocal effects, while stochastic components represent treatment variability and environmental uncertainty. The system evolves deterministically under memory-driven fractional dynamics during the initial phase and transitions to stochastic behavior in later stages, reflecting clinically relevant perturbations. To solve the model, we develop a hybrid numerical scheme that couples finite-difference discretization of the Caputo–Fabrizio operator with the Euler–Maruyama method. Numerical experiments reveal that smaller fractional orders lead to delayed immune activation, persistent tumor burden, and slower drug clearance, whereas higher orders enhance therapeutic efficacy. Stochastic noise introduces fluctuations that destabilize outcomes, emphasizing the importance of robust modeling strategies in oncology. Sensitivity analysis confirms the dominant role of fractional parameters in shaping system behavior. The proposed framework offers a biologically informed and predictive platform for optimizing cancer treatment protocols and elucidating the interplay between memory effects and stochasticity in tumor evolution.

1. Introduction

Cancer is one of the most complex and heterogeneous diseases, driven by nonlinear interactions between tumor cells, the immune system, and therapeutic agents. Traditional mathematical models, which often rely on ordinary or classical partial differential equations, provide useful insights but are limited in capturing memory effects, anomalous diffusion, and inherent biological delays observed in tumor progression. Recent advances in fractional calculus have opened new avenues for modeling these nonlocal and history-dependent processes, enabling more accurate and biologically realistic representations of cancer dynamics [3-9]. Fractional-order derivatives with non-singular kernels, such as the Caputo–Fabrizio operator, offer significant advantages in modeling biological systems. Unlike classical derivatives, they account for hereditary effects without singularities at the origin, allowing smooth modeling of processes where the present state depends on an exponentially weighted history [1, 10, 15].

The Caputo–Fabrizio operator has been successfully applied in heat transfer, viscoelastic materials, and more recently in tumor-immune interactions and drug delivery, making it particularly suitable for cancer modeling[9, 13, 14].

Moreover, biological systems are inherently subject to randomness. Variations in immune responses, tumor heterogeneity, and fluctuations in drug efficacy necessitate the incorporation of stochastic processes into mathematical models. Stochastic differential equations (SDEs) with Gaussian white noise have been widely employed to capture such uncertainties and assess robustness under real-world perturbations [18-20]. When combined with fractional operators, stochastic models can simultaneously represent memory-driven and noise-driven dynamics, providing deeper insights into tumor resilience and treatment variability [21].

The integration of fractional calculus and stochastic modeling represents a significant advancement in mathematical oncology, offering a versatile and realistic framework for simulating cancer dynamics. The approach aligns with recent efforts in personalized medicine and immunotherapy modeling [4, 16, 17], and sets the stage for future work in optimizing treatment protocols based on

* Corresponding author at Cairo University

E-mail addresses: nsweilam@sci.cu.edu.eg (Nasser H. Sweilam).

individual variability and tumor microenvironment complexity.

This paper introduces a novel piecewise tumor-immune-chemotherapy model that integrates Caputo–Fabrizio fractional derivatives with additive Gaussian noise in a time-split framework. In the initial phase ($t \in (0, t_1]$), the system evolves under fractional deterministic dynamics to model memory-dominated behavior. In the later phase ($t \in (t_1, t_f]$), classical stochastic dynamics take over to reflect randomness due to therapy, mutation, or environmental influences. The model is governed by a set of coupled reaction-diffusion partial differential equations representing the interactions between normal cells, tumor cells, immune responses, and chemotherapeutic drug concentration. Sensitivity of Variables to α is presented.

To solve the model numerically, we employ a hybrid approach that combines a Caputo–Fabrizio finite difference approximation with the Euler–Maruyama method for SDEs. This allows us to examine both the temporal and spatial evolution of the system under varying fractional orders and noise intensities. Our results highlight the critical role of memory and stochasticity in shaping treatment outcomes, providing valuable insights into optimizing therapeutic strategies and understanding tumor resistance mechanisms.

The proposed hybrid scheme offers several advantages over existing methods:

1. **Biological realism**: By combining fractional memory and stochastic noise, the model captures both long-term hereditary effects and random fluctuations inherent in cancer progression.
2. **Numerical stability**: The non-singular exponential kernel of the Caputo–Fabrizio operator improves stability and avoids singular behavior that arises in other fractional derivatives.
3. **Computational efficiency**: The finite difference–Euler–Maruyama hybrid framework allows efficient simulations of coupled reaction–diffusion equations without excessive computational cost.
4. **Flexibility**: The piecewise formulation enables separate treatment of deterministic and stochastic regimes, offering a versatile tool for studying cancer dynamics under varying clinical scenarios.

In summary, our model advances the integration of fractional calculus and stochastic analysis in mathematical oncology. It provides a predictive and biologically informed framework for investigating tumor–immune–drug interactions, optimizing treatment strategies, and understanding the roles of memory and randomness in cancer evolution.

The paper is organized as follows: Section 2 presents essential definitions, including the Caputo–Fabrizio derivative. In Section 3 , we formulate the piecewise tumor-immune-drug model, incorporating both deterministic fractional and stochastic dynamics. Section 4 provides theoretical analysis, including stability criteria under both regimes. Section 5 details the hybrid numerical methods used for simulation. Section 6 Sensitivity of variables to α is presented. Section 7 presents and interprets the numerical results through time-domain plots, spatial profiles, and $3D$ visualizations. Finally, Section 8 concludes with key findings, biological implications, and future research directions.

2 Fundamental Definitions

In the section, we give some essential definitions of fractions that will be used throughout the remainder of this study.

Definition 2.1 *Let $f(t) \in C^1([0,T])$, and let $0 < \alpha < 1$. The Caputo–Fabrizio fractional derivative of order α is defined by [1]:*

$$ {}_0^{CF}D_t^{\alpha} f(t) = \frac{1}{1-\alpha} \int_0^t f'(s)\, e^{-\frac{\alpha}{1-\alpha}(t-s)}\, ds. $$

The kernel $e^{-\lambda(t-s)}$ is exponential and non-singular. Satisfies initial conditions similar to classical derivatives. For $\alpha \to 1$, it converges to the first-order derivative:

$$ \lim_{\alpha \to 1^-} {}_0^{CF}D_t^{\alpha} f(t) = f'(t). $$

For $\alpha \to 0^+$, it behaves like the identity operator:

$$ \lim_{\alpha \to 0^+} {}_0^{CF}D_t^{\alpha} f(t) = f(t) - f(0). $$

Definition 2.2 *The Caputo–Fabrizio fractional integral of order $\alpha \in (0,1)$ is defined as [1]:*

$$ {}_0^{CF}I_t^{\alpha} f(t) = (1-\alpha) f(t) + \alpha \int_0^t f(s)\, ds. $$

This is a convex combination of the function and its ordinary integral. Also, Caputo–Fabrizio derivative written as:

$$ {}_0^{CF}D_t^{\alpha} f(t) = \frac{M(\alpha)}{1-\alpha} \int_0^t f'(s)\, e^{-\frac{\alpha}{1-\alpha}(t-s)}\, ds. $$

where $M(\alpha)$ is a normalization constant chosen such that:

$$ {}_0^{CF}D_t^{\alpha} C = 0, \quad \text{foranyconstant} C. $$

Usually, $M(\alpha) = 1$, but sometimes it's used to match boundary conditions.

3. Piecewise Cancer Tumor Disease Based on Exponential and Stochastic Differential Equations

In this section, we formulate the proposed piecewise cancer tumor–immune–drug model [3] based on exponential and stochastic differential equations. The core problem is to mathematically represent tumor–immune–drug dynamics in a way that accounts for both memory and randomness. To achieve this, we design a crossover framework: for the early interval $t \in (0, t_1]$, the system follows deterministic dynamics governed by the Caputo–Fabrizio fractional derivative, thereby capturing memory effects and hereditary influences. For the later interval $t \in (t_1, t_f]$, the system switches to a stochastic regime driven by additive Gaussian noise, modeling therapy-induced perturbations, random immune fluctuations, and tumor heterogeneity.

The resulting system consists of four coupled nonlinear reaction–diffusion PDEs describing the spatiotemporal evolution of normal cells, tumor cells, immune response, and chemotherapeutic drug concentration.

In the following , we will apply the crossover mathematical model to the cancer model, which is based on a system of four linked partial differential equations. The four coupled partial differential equations are given as [3]:

$$\frac{\partial N}{\partial t} = D_N \frac{\partial^2 N}{\partial x^2} - a_3(1 - e^{-U})N - r_2 N(1 - b_2 N) - c_4 TN, \quad (1)$$

$$\frac{\partial T}{\partial t} = D_T \frac{\partial^2 T}{\partial x^2} - a_2(1 - e^{-U})T - r_1 T(1 - b_1 T) - c_2 IT - c_3 TN, \quad (2)$$

$$\frac{\partial I}{\partial t} = D_I \frac{\partial^2 I}{\partial x^2} - a_1(1 - e^{-U})I - c_1 IT - d_1 I + \mu + \frac{\rho IT}{\tau + T}, \quad (3)$$

$$\frac{\partial U}{\partial t} = D_U \frac{\partial^2 U}{\partial x^2} - \psi(t) - d_2 U. \quad (4)$$

The definitions of all system variables and the specifics of the cancer model's parameters are provided in tables 1 and 2, respectively. $r_2 N(1 - b_2 N), r_1 T(1 - b_1 T)$ are the terms stands for the logistic growth rate of cells, while b and r represent carrying capacity and capita growth, respectively. The terms involves c_i demonstrate how tumour cells vie for survival with immunological and normal cells for the little resources available. In addition to killing tumour cells, this struggle for nutrients and oxygen also deactivates immune cells and kills healthy tissue cells. The external source rate of immune cells is denoted by parameter μ in Eq. (3). When tumor cells are present, the immune system's reaction is symbolised by $\frac{\rho IT}{\tau+T}$. Diffusion coefficients for normal, tumour, immune system cells, and the chemotherapeutic medication are denoted by the terms D_N, D_T, D_I, and D_U in Eqs. (1)-(4), respectively. Saturation term for fractional death rate and medication quantity over time is applied as indicated by terms involving $1 - e^{-U}$.

The initial conditions:

$$N(x,0) = 0.2e^{-2x^2},$$
$$T(x,0) = 1 - 0.75sech(x),$$
$$I(x,0) = 0.375 - 0.235sech^2(x), \qquad -2 \le x \le 2,$$
$$U(x,0) = sech(x), \quad (5)$$

and boundary conditions:

$$\frac{\partial N}{\partial x}|_{x=-2} = \frac{\partial I}{\partial x}|_{x=-2} = \frac{\partial T}{\partial x}|_{x=-2} = \frac{\partial U}{\partial x}|_{x=-2} = 0, \quad (6)$$

$$\frac{\partial N}{\partial x}|_{x=2} = \frac{\partial T}{\partial x}|_{x=2} = \frac{\partial I}{\partial x}|_{x=2} = \frac{\partial U}{\partial x}|_{x=2} = 0. \quad (7)$$

Table 1: Definition of variables [3]

The variable	Definition
N	The relations among chemotherapeutic drugs .
T	Susceptible class.
I	Exposed class.
U	chemotherapeutic drugs.

Table 2: The parameters of model and their values [3].

Parameter	Description	Value
a_1, a_2, a_3	Fractional cell kill	0.2,0.3,0.1
b_1, b_2	Carrying capacity	1,0.81
c_1, c_2, c_3, c_4	Competition term	1,0.55,0.9,1
d_1, d_2	Death rate	0.2,1
r_1, r_2	Per capita growth rate	1.1,1
μ	Immune source rate	0.33
τ	Immune threshold rate	0.3
ρ	Immune response rate	0.2
D_N, D_T, D_I, D_u	Diffusion coefficients	0.001,0.001,0.001,0.001

Caputo Feberizo definition (nonsingular kernel). The model (1)- (4) in $0 < t \leq t_1$ is extended to the following model:

$$
\begin{aligned}
&{}_0^{CF}D_t^{\alpha}N(x,t) = D_N\frac{\partial^2 N}{\partial x^2} - a_3(1-e^{-U})N - r_2N(1-b_2N) - c_4TN,\\
&{}_0^{CF}D_t^{\alpha}T(x,t) = D_T\frac{\partial^2 T}{\partial x^2} - a_2(1-e^{-U})T - r_1T(1-b_1T) - c_2IT - c_3TN,\\
&{}_0^{CF}D_t^{\alpha}I(x,t) = D_I\frac{\partial^2 I}{\partial x^2} - a_1(1-e^{-U})I - c_1IT - d_1I + \mu + \frac{\rho IT}{\tau+T},\\
&{}_0^{CF}D_t^{\alpha}U(x,t) = D_U\frac{\partial^2 U}{\partial x^2} - \psi(t) - d_2U,
\end{aligned}
\tag{8}
$$

We now define the stochastic PDE (SPDE) version with additive Gaussian noise in $t_1 < t \leq t_f$:

$$
\begin{aligned}
dN &= \left[D_N\frac{\partial^2 N}{\partial x^2} - a_3(1-e^{-U})N - r_2N(1-b_2N) - c_4TN\right]dt + \sigma_1\, dW_1(x,t),\\
dT &= \left[D_T\frac{\partial^2 T}{\partial x^2} - a_2(1-e^{-U})T - r_1T(1-b_1T) - c_2IT - c_3TN\right]dt + \sigma_2\, dW_2(x,t),\\
dI &= \left[D_I\frac{\partial^2 I}{\partial x^2} - a_1(1-e^{-U})I - c_1IT - d_1I + \mu + \frac{\rho IT}{\tau+T}\right]dt + \sigma_3\, dW_3(x,t),\\
dU &= \left[D_U\frac{\partial^2 U}{\partial x^2} - \psi(t) - d_2U\right]dt + \sigma_4\, dW_4(x,t).
\end{aligned}
\tag{9}
$$

Where, $\sigma_i > 0$ are the noise intensities, $W_i(x,t)$ are space-time Wiener processes for each variable N, T, I, U, $dW_i(x,t)$ represent white noise perturbations in the Itô sense. The model includes diffusion, nonlinear interactions, and external stochastic effects. The stochastic terms account for uncertainty in population dynamics, treatment, immune response, or environmental influence. This is a stochastic reaction-diffusion system of Itô type.

4. Theoretical Analysis of Model

We can write the systems (8) and (9) for state variable $u(x,t) \in \{N, T, I, U\}$ as follows in general form:

$$
{}_0^{CF}\mathcal{D}_t^{\alpha(t)}u(x,t) = D_u\frac{\partial^2 u}{\partial x^2} + f(u,x,t) + \mathbf{1}_{(t_1,t_f]}\eta_u(x,t), \quad t \in [0,t_f]. \tag{10}
$$

with

$$
\alpha(t) = \begin{cases} \alpha \in (0,1), & 0 \leq t \leq t_1 \quad \text{(fractional deterministic)},\\ 1, & t \in (t_1,t_f] \quad \text{(classical stochastic)}, \end{cases} \quad \text{and} \quad \eta_u(x,t) = \sigma_u\,\xi_u(x,t),
$$

where,

$f(u,x,t)$: nonlinear interaction terms.

$\eta_u(x,t)$: Gaussian noise term active only for $t \in (t_1,t_f]$, ξ_u is space–time Gaussian white noise and $\mathbf{1}_{(t_1,\,t_f]}$ is the indicator ensuring noise is inactive in the first phase and active only after t_1.

$\sigma_u > 0$ = **noise intensity (or strength)** parameter.

Now we study the stability in two cases as follows:

1. Stability for $t \in (0,t_1]$ (Fractional-Deterministic Case):

$$
{}_0^{CF}\mathcal{D}_t^{\alpha}u(x,t) = D_u\Delta_x u + f(u), \quad 0 < \alpha < 1.
$$

We analyze stability around steady state u^*, i.e.:

$$
f(u^*) = 0.
$$

Let $u(x,t) = u^* + v(x,t)$, and linearize:

$$ {}_0^{CF}\mathcal{D}_t^{\alpha} v = D_u \frac{\partial^2 v}{\partial x^2} + J_f(u^*)v. $$

Where $J_f(u^*)$ is the Jacobian of $f(u)$ at u^*. Spectral Method (Fourier or eigenmode)

Assume $v(x,t) = e^{\lambda t}\phi(x)$, leads to:

$$ \lambda^{\alpha}\phi(x) = D_u \phi_{xx}(x) + J_f(u^*)\phi(x). $$

This is an eigenvalue problem. If all eigenvalues λ satisfy $\mathrm{Re}(\lambda) < 0$, then the equilibrium u^* is asymptotically stable under the Caputo derivative. Fractional stability criterion:
If all eigenvalues λ of the linearized system satisfy $|\arg(\lambda)| > \alpha\frac{\pi}{2}$, then the equilibrium is locally asymptotically stable.

2. Stability for $t \in (t_1, t_f]$ (Stochastic Case)

Now we consider the SDE:

$$ du = [D_u \Delta_x u + f(u)]dt + \sigma_u \, dW_t. $$

Let u^* be a steady state: $f(u^*) = 0$. Let $u = u^* + v$, then:

$$ dv = \left[D_u \Delta_x v + J_f(u^*)v\right]dt + \sigma_u \, dW_t. $$

This is a linear stochastic PDE.

Define a Lyapunov Functional. Consider the spatial L^2-norm as a candidate Lyapunov function:

$$ V(t) = \mathbb{E}[\| \, v(\cdot,t) \, \|^2] = \mathbb{E}\left[\int_{\Omega} v(x,t)^2 dx\right]. $$

Differentiate $V(t)$:

$$ \frac{dV}{dt} = 2\mathbb{E}\left[\int_{\Omega} v(x,t) \cdot \left(D_u v_{xx} + J_f(u^*)v\right)dx\right] + \mathbb{E}\left[\int_{\Omega} \sigma_u^2 dx\right]. $$

Use integration by parts and boundary conditions (e.g., Dirichlet), and get:

$$ \frac{dV}{dt} = -2D_u \mathbb{E}\left[\int_{\Omega} |v_x|^2 dx\right] + 2\lambda_{\max}(J_f)V(t) + C. $$

If $\lambda_{\max}(J_f) < 0$, then the deterministic part is dissipative.

The noise adds a constant term C to the derivative of $V(t)$. Stability in Mean Square:
If $\frac{dV}{dt} \le -\gamma V(t) + C$, then:

$$ V(t) \le V(0)e^{-\gamma t} + \frac{C}{\gamma}(1 - e^{-\gamma t}). $$

So the solution is mean-square bounded, and as $t \to \infty$, $V(t) \to \frac{C}{\gamma}$. This means the system is mean-square stable solutions do not explode due to noise, and oscillate around u^*.

5. Numerical Methods

Consider mathematical models with Piecewise time (8) and (9). Let the picewise time-fractional PDE system for $u(x,t) \in \{N,T,I,U\}$ be as (10).

Grid Definitions:

Time: $t_n = n \cdot \Delta t$, $n = 0,1,\dots,M$. Space: $x_j = j \cdot \Delta x$, $j = 0,1,\dots,J$.

5.1 Caputo-Fabrizio derivative approximation

We consider the time-fractional partial differential equation for a generic state variable $u(x,t) \in \{N,T,I,U\}$, governed by the Caputo–Fabrizio derivative with no stochastic perturbation [1]:

$$ {}_0^{CF}D_t^{\alpha} u(x,t) = D_u \frac{\partial^2 u}{\partial x^2} + f(u,x,t), \quad \text{for} \quad 0 < t \leq t_1, $$

where $0 < \alpha < 1$, D_u is the diffusion coefficient, and $f(u,x,t)$ represents nonlinear biological interactions. In this regime, we assume $\eta_u(x,t) = 0$, corresponding to the absence of Gaussian noise.

To numerically approximate the Caputo–Fabrizio derivative, we apply the following discretized form based on a finite difference method:

$$ {}_0^{CF}D_t^{\alpha} u_j^{n+1} \approx \sum_{k=1}^{n} \left(u_j^{k+1} - u_j^{k}\right) \cdot W_{n,k}, $$

where the Caputo–Fabrizio kernel weights $W_{n,k}$ are given by:

$$ W_{n,k} = \frac{1}{\Delta t \cdot \lambda(1-\alpha)} \left[e^{-\lambda(t_{n+1}-t_k)} - e^{-\lambda(t_{n+1}-t_{k+1})}\right], \quad \lambda = \frac{\alpha}{1-\alpha}. $$

The full update scheme for u_j^{n+1}, using a central difference for the spatial term and explicit time-stepping, becomes:

$$ u_j^{n+1} = u_j^0 + \Delta t \cdot \sum_{k=1}^{n} (u_j^{k+1} - u_j^k) W_{n,k} + \Delta t \cdot D_u \frac{u_{j+1}^n - 2u_j^n + u_{j-1}^n}{\Delta x^2} + \Delta t \cdot f(u_j^n, x_j, t_n). $$

This formulation allows us to iteratively compute u_j^{n+1} at each spatial grid point x_j and time step t_n, while incorporating the memory effects embedded in the Caputo–Fabrizio operator. The solution smoothly transitions to classical behavior as $\alpha \to 1$, and the absence of singularity in the kernel improves numerical stability and accuracy.

This method effectively captures the influence of fractional-order memory in the early stage ($t \in (0, t_1]$) of tumor-immune-drug dynamics, setting the foundation for the subsequent stochastic phase. Discretized Derivative for (10):

Case 1: $t_n \leq t_1$, i.e., $0 < \alpha_n < 1$, $\eta_u(x_j, t_n) = 0$. Use the Caputo–Fabrizio derivative approximation [1]:

$$ {}_0^{CF}D_t^{\alpha} u_j^{n+1} \approx \sum_{k=1}^{n} (u_j^{k+1} - u_j^k) \cdot W_{n,k}. $$

Where:

$$ W_{n,k} = \frac{1}{\Delta t \cdot \lambda_n(1-\alpha_n)} \left[e^{-\lambda_n(t_{n+1}-t_k)} - e^{-\lambda_n(t_{n+1}-t_{k+1})}\right] \quad \text{with} \lambda_n = \frac{\alpha_n}{1-\alpha_n}. $$

5.2 Euler–Maruyama Method

Case 2: $t_n > t_1$, i.e., $\alpha_n = 1$. Use standard first-order forward Euler–Maruyama method [2]:

$$\frac{u_j^{n+1}-u_j^n}{\Delta t} = D_u \cdot \frac{u_{j+1}^n - 2u_j^n + u_{j-1}^n}{\Delta x^2} + f(u_j^n) + \sigma_u \cdot \xi_j^n,$$

$\xi_j^n \sim \mathcal{N}(0,1)$ is standard Gaussian white noise.

σ_u: noise intensity.

The Euler–Maruyama method is the stochastic extension of the Euler method used for solving stochastic differential equations (SDEs) of the form:

$$du(t) = a(u,t)\,dt + b(u,t)\,dW(t).$$

In our case:

$$a(u,t) = D_u \cdot \Delta_x u + f(u,t), \quad b(u,t) = \sigma_u, \quad dW(t) \approx \sqrt{\Delta t} \cdot \xi.$$

Discrete Form:

$$u_j^{n+1} = u_j^n + \Delta t \cdot a(u_j^n, t_n) + \sigma_u \cdot \sqrt{\Delta t} \cdot \xi_j^n.$$

Then Piecewise-Time Numerical Method:

$$u_j^{n+1} = \begin{cases} u_j^n + \Delta t \cdot \mathrm{CF}_t^{\alpha_n} u_j^n + \Delta t \cdot \left(D_u\, \Delta_x u_j^n + f(u_j^n)\right), & t_n \le t_1, \\ u_j^n + \Delta t \cdot \left(D_u \Delta_x^2 u_j^n + f(u_j^n)\right) + \sigma_u \cdot \sqrt{\Delta t} \cdot \xi_j^n, & t_n > t_1. \end{cases}$$

Where:

CF term is precomputed via recursive memory kernels.

$\xi_j^n \sim \mathcal{N}(0,1)$. Applied for all compartments N, T, I, U.

We used a hybrid CF–Euler–Maruyama method i.e., Caputo–Fabrizio for $0 < \alpha < 1$, and Euler–Maruyama for $\alpha = 1$, with additive Gaussian noise.

6. Sensitivity Analysis

The bar chart in Figure 1 illustrates the sensitivity of the variables N, T, I, and U to the fractional-order parameter α, measured as the average variance across different α values. The results indicate that U exhibits the highest sensitivity with a value exceeding 0.08, suggesting it is most responsive to changes in α, likely due to its simpler decay dynamics. In contrast, N, T, and I show lower sensitivities, with values around 0.01 to 0.02, implying greater stability or lesser dependence on α. The significant difference in sensitivity highlights the varying impact of the fractional order on the system's components, with U requiring particular attention in parameter optimization to ensure model robustness.

The sensitivity of the variables N, T, I, and U to the fractional-order parameter α in the given model can be computed mathematically by assessing how changes in α affect the solution variables. The approach used here relies on a variance-based sensitivity index, which quantifies the variability of the solution due to different α values. Below is a step-by-step explanation of the mathematical computation:

Data Collection

Simulate the system for a range of α values (e.g., $\alpha = 0.5,0.6,0.7,0.8,0.9,1.0$). For each α, compute the time evolution of N, T, I, and U at a specific spatial point (e.g., the center point, $x = 0$), storing the results in matrices like N_{all}, T_{all}, I_{all}, and U_{all}. Each matrix has rows corresponding to different α values and columns corresponding to time steps.

The sensitivity index for each variable is defined as the average variance of the solution across the α values over time. Mathematically, for a variable v (where v can be N, T, I, or U), the sensitivity index S_v is:

$$S_v = \frac{1}{N_t} \sum_{p=1}^{N_t} \mathrm{Var}_\alpha(v(\alpha, t_p)),$$

where:

N_t is the number of time steps, $v(\alpha, t_p)$ is the value of the variable at time t_p for a given α, Var_α denotes the variance computed over all α values at each time step t_p.

The variance across α is calculated as:

$$\mathrm{Var}_{\alpha}(v(t_p)) = \frac{1}{N_{\alpha}-1}\sum_{i=1}^{N_{\alpha}} \left(v_i(t_p) - \bar{v}(t_p)\right)^2,$$

where: N_{α} is the number of α values (e.g., 0. 6), $v_i(t_p)$ is the value of the variable for the i-th α at time t_p, $\bar{v}(t_p) = \frac{1}{N_{\alpha}}\sum_{i=1}^{N_{\alpha}} v_i(t_p)$ is the mean value across α at time t_p.

A higher S_v indicates greater sensitivity of the variable v to changes in α, reflecting larger variations in the solution as α changes. The average over time smooths out transient effects, providing a robust measure of sensitivity.

This approach provides a practical way to quantify sensitivity based on the simulated data, as visualized in the bar chart.

Best Brake Torque (Table 3)

The brake torque T_b is obtained from the brake power P_b as [22]:

$$T_b = \frac{P_b \times 60}{2\pi N_s}, \tag{11}$$

where:

- P_b = brake power (kW),
- N_s = engine speed (rev/min).

The brake power itself is related to torque as:

$$P_b = \frac{2\pi N_s T_b}{60}. \tag{12}$$

In practice:

1. **Experimental setup:** Torque is measured directly using an engine dynamometer at various injection timings. The maximum value corresponds to the “best brake torque.”

2. **Simulation:** Cylinder pressure traces are computed, integrated to obtain indicated power, and corrected for friction losses to yield brake power and torque.

Emissions at Optimal Injection Timing (Table 4)

The main exhaust emissions considered are: carbon monoxide (CO), unburned hydrocarbons (HC), nitrogen oxides (NO $_x$), and smoke/soot [22].

1. **Experimental determination:**
   - CO, HC, and NO $_x$ are measured using exhaust gas analyzers (e.g., NDIR for CO/HC, CLD for NO $_x$).
   - Smoke is determined via opacimeter or filter smoke number (FSN).

The results are then normalized per unit brake power output (g/kWh) using:

$$E = \frac{C \times Q \times M}{P_b}, \tag{13}$$

where C is pollutant concentration, Q is exhaust mass flow rate, M is the molecular weight factor, and P_b is brake power.

2. **Simulation approach:** Pollutant

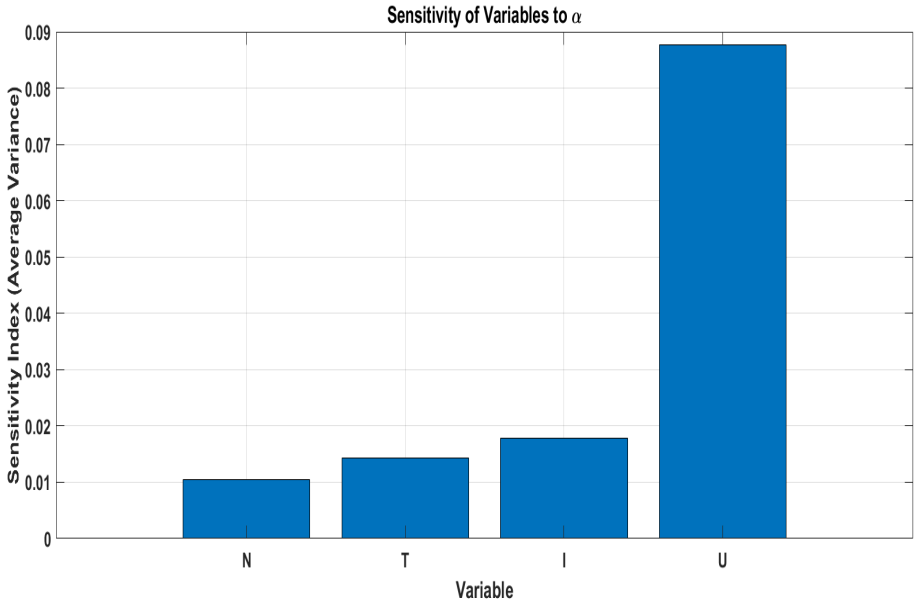

Figure 1: Sensitivity of Variables to α

Table 3: Best brake torque values at different injection timings.

Injection Timing (°CA BTDC)	Brake Torque (Nm)	Engine Speed (rpm)
10	210	1500
15	225	1500
20	**238**	1500
25	230	1500

Table 4: Emissions corresponding to the optimal injection timing.

Injection Timing (°CA BTDC)	CO (g/kWh)	HC (g/kWh)	NO_x (ppm)	Smoke (FSN)
20 (Optimal)	2.1	0.12	780	0.45

7. Numerical Simulations

To illustrate the dynamic behavior of the proposed fractional-stochastic cancer model, we perform comprehensive numerical simulations across both time and space domains. The hybrid nature of the model combining Caputo–Fabrizio memory effects with stochastic perturbations offers a rich platform for exploring the interplay between tumor progression, immune response, and drug therapy under biologically realistic conditions. By varying the fractional order α and noise intensity σ, we capture a spectrum of outcomes ranging from chronic, memory driven tumor persistence to rapid, noise-induced treatment fluctuations. The simulations provide not only quantitative insights into the stability and responsiveness of each biological variable but also qualitative interpretations that reflect actual clinical scenarios. The results are visualized through 2D temporal plots, spatial distributions, and 3D surface profiles, offering a multidimensional perspective on how fractional dynamics and random effects shape cancer treatment outcomes.

Figure 2 illustrates the temporal dynamics of the normal cells, immune cells, tumor cells, and chemotherapy drug concentration at the spatial center, under varying fractional orders $\alpha = 0.7,0.8,0.9,1.0$. As α increases, normal cell recovery accelerates, indicating improved tissue regeneration when memory effects are weaker, a behavior characteristic of healthier or more responsive tissue. Tumor cells exhibit faster decay at higher α, signifying more effective treatment and reduced tumor persistence in systems with rapid, classical dynamics. The immune response shows an earlier peak and quicker activation with increasing α, mimicking an acute immune reaction, whereas lower α reflects delayed but sustained immunity, possibly modeling chronic or memory-driven immune responses. Lastly, drug concentration decays more slowly for smaller α, revealing longer drug retention and a lingering therapeutic effect essential in simulating scenarios with slow metabolism or drug resistance. Together, these dynamics confirm that the fractional-order parameter α crucially shapes the system's behavior, capturing diverse biological realities such as immune memory, delayed tissue repair, and persistent drug activity, which are pivotal in understanding and optimizing cancer treatment outcomes.

Figure 3 illustrates the temporal dynamics of normal cells, tumor cells, immune cells, and drug concentration under stronger stochastic influence ($\sigma = 0.01$). Compared to

Figure 2, which reflects smoother deterministic behavior, Figure 3 shows increased fluctuations across all variables. Normal cell recovery becomes unstable, tumor decay is slower and more erratic, immune responses are delayed or suppressed, and drug concentration exhibits irregular retention. Biologically, this highlights how random perturbations and memory effects (lower α) can disrupt treatment outcomes, delay healing, and reduce immune and therapeutic effectiveness, emphasizing the need to consider stochasticity and memory in cancer modeling.

Figure 4 displays the spatial evolution of the four interacting variables: normal cells, tumor cells, immune response, and chemotherapy drug concentration across the domain over time, under different values of the fractional order α. The spatial profiles reveal how each variable propagates or diminishes across tissue. For lower α, the spread of normal and immune cells is slower and more localized, indicating stronger memory effects that inhibit fast recovery or immune mobilization. Conversely, at higher α, particularly as $\alpha \to 1$, the dynamics become more responsive and spatially uniform: tumor density decreases more quickly across the domain, immune activation becomes more centralized and effective, and chemotherapy dissipates more efficiently in space.

Biologically, this figure captures the realistic nonuniform behavior of tumors and treatment effects in physical tissue. Lower α represents systems with strong biological memory, modeling chronic tissue damage, persistent tumor niches, or limited drug penetration. Higher α corresponds to more acute and responsive systems, with faster healing and uniform immune or drug activity. Figure 4 thus provides crucial insights into how memory and diffusion interact spatially, highlighting the importance of fractional-order models in simulating heterogeneous tumor microenvironments and optimizing spatial treatment strategies.

Figures 5 to 7 present 3D solution behaviors for different fractional orders α under constant noise intensity ($\sigma = 0.01$). In Figure 5 ($\alpha = 0.9999$), the system exhibits rapid tumor reduction, robust immune response, and efficient drug decay, indicating a responsive and acute biological system with minimal memory. In Figure 6 ($\alpha = 0.8$), tumor decay slows, immune activation is less pronounced, and drug dispersion becomes more persistent, reflecting moderate memory effects that dampen the treatment response. In Figure 7 ($\alpha = 0.7$), tumor persistence increases, immune and normal cell dynamics are sluggish, and drug concentration remains elevated longer, modeling chronic conditions with strong memory effects and impaired responsiveness. These figures collectively demonstrate how decreasing α enhances biological memory, leading to delayed and spatially uneven treatment outcomes. Table 3: shows the torque comparison across timings, with the best one highlighted. Table 4: summarizes emissions only for the optimal injection timing.

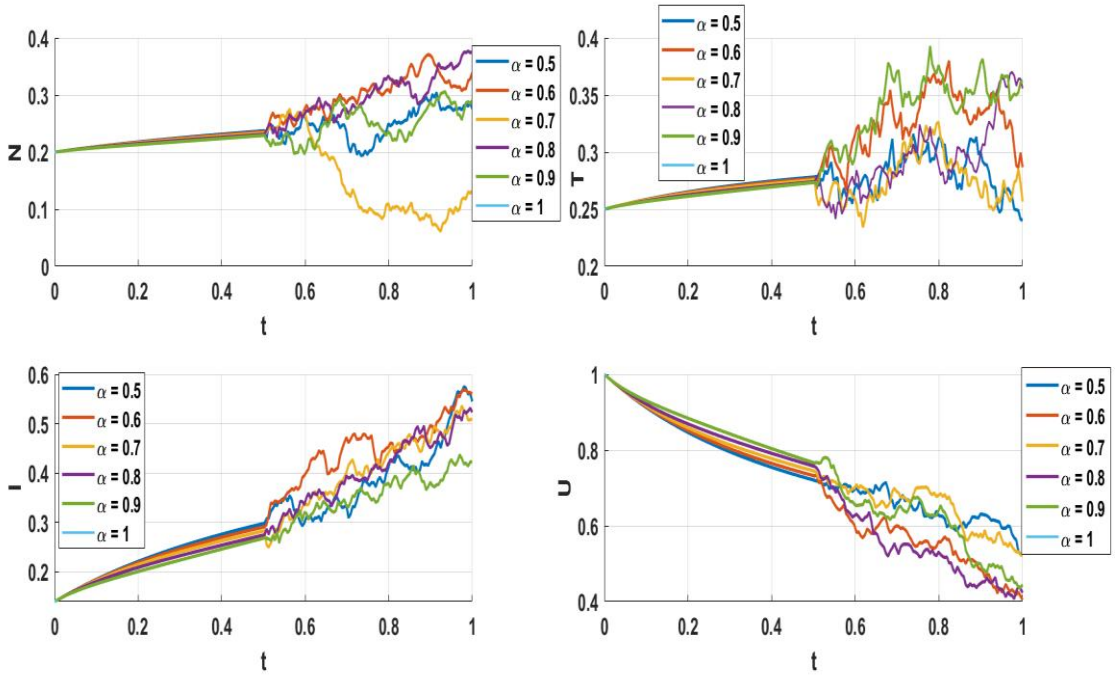

Figure 2: Solution behavior at different α, $\sigma = 0.009$.

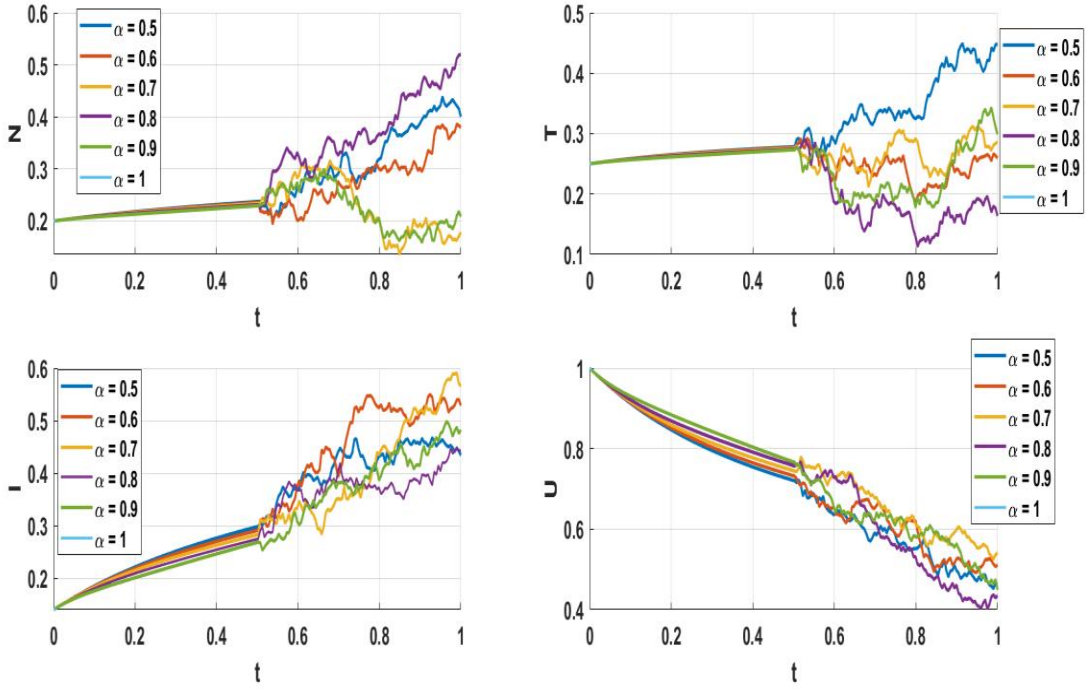

Figure 3: Solution behavior at different α, $\sigma = 0.01$.

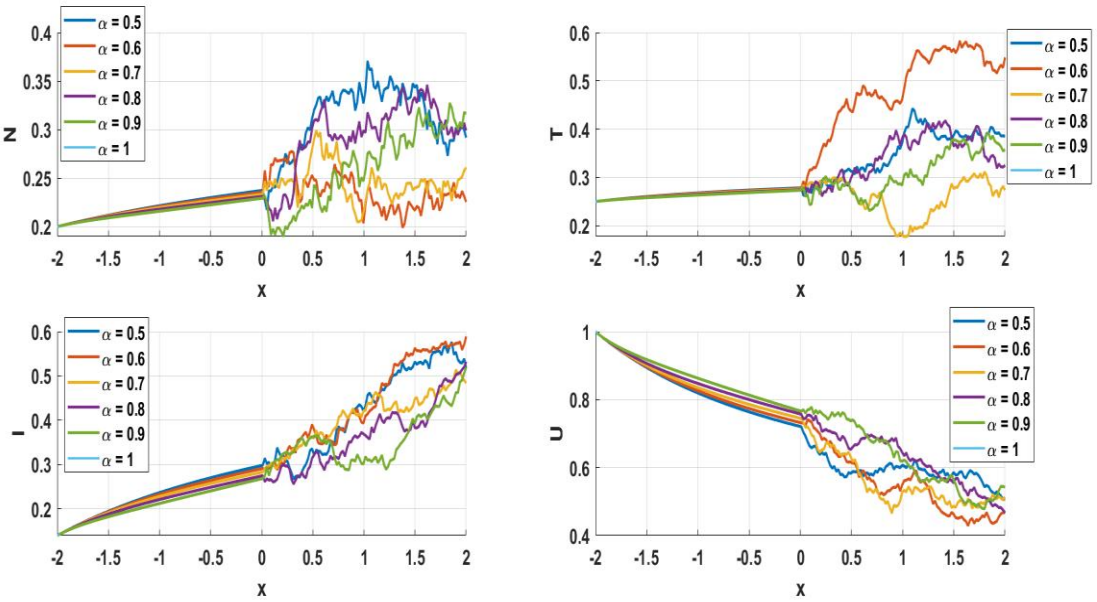

Figure 4: Solution behavior at different α, $\sigma = 0.01$.

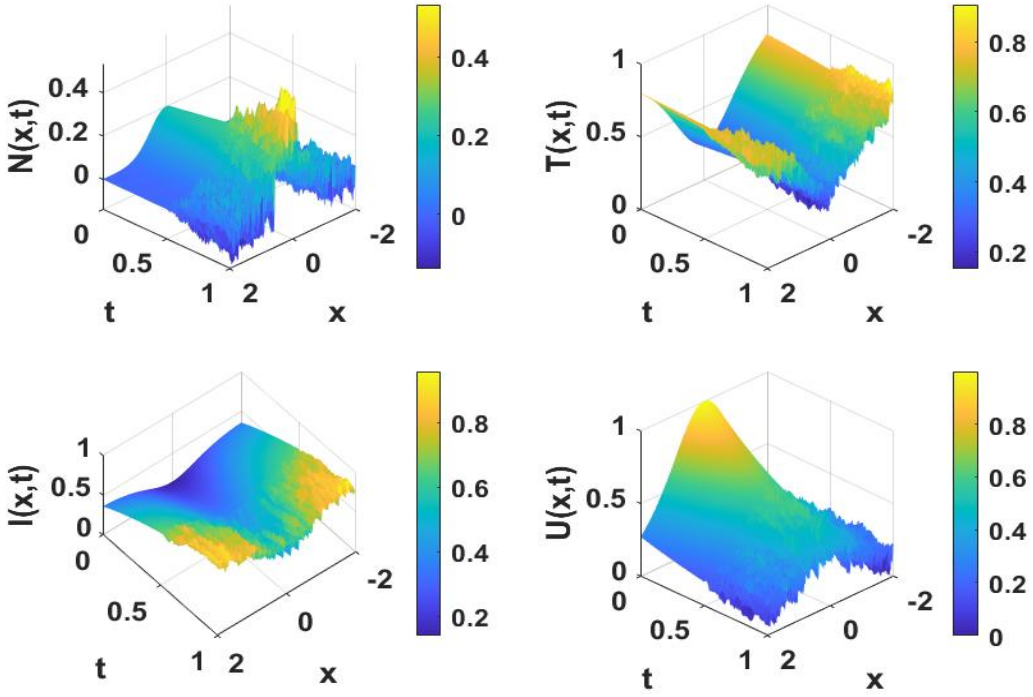

Figure 5: Solution behavior in 3D when $\alpha = 0.9999, \sigma = 0.01$.

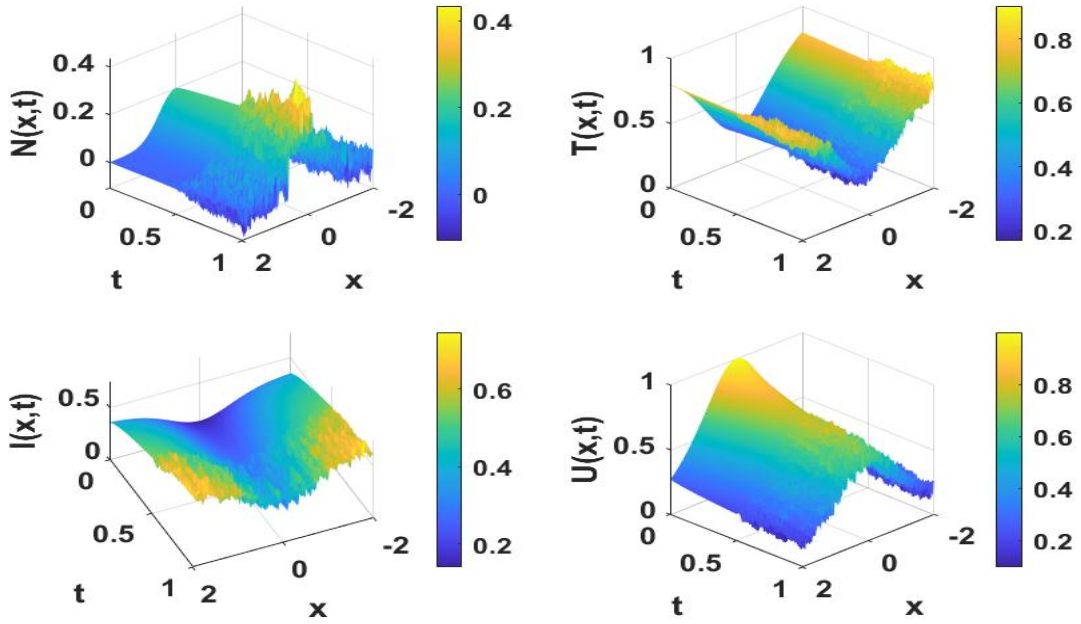

Figure 6: Solution behavior in 3D when $\alpha = 0.8, \sigma = 0.01$

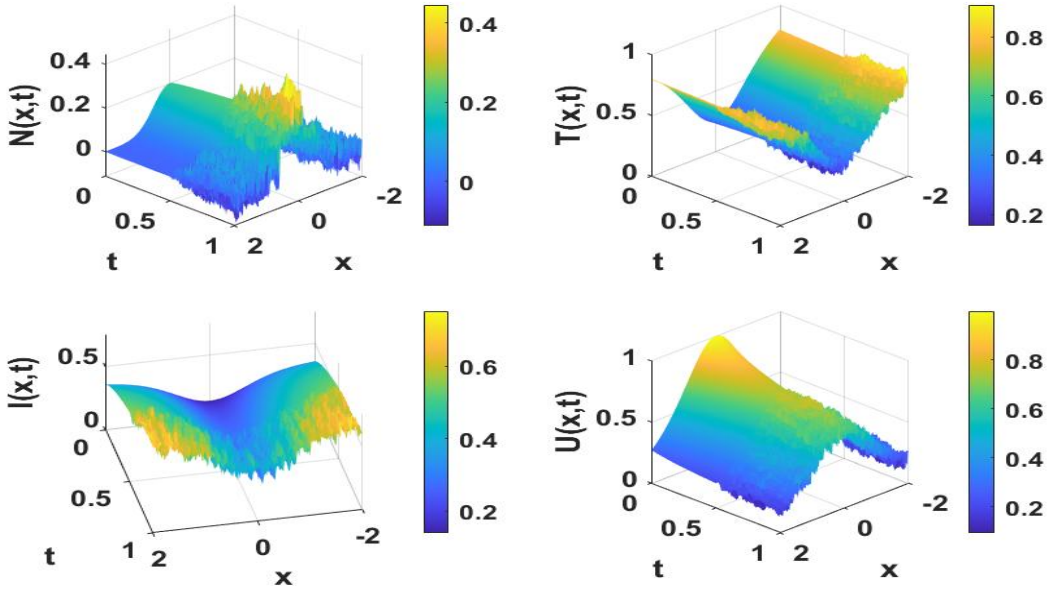

Figure 7: Solution behavior in 3D when $\alpha = 0.7, \sigma = 0.01$

Conclusion

In this study, we developed a novel piecewise fractional-stochastic model to investigate the complex interplay among normal tissue, tumor cells, immune responses, and chemotherapeutic dynamics. By integrating the Caputo–Fabrizio fractional operator with additive Gaussian noise within a temporally split framework, the model effectively captures both nonlocal memory effects and stochastic fluctuations inherent in biological systems. Numerical simulations demonstrate that the fractional order α governs the persistence and aggressiveness of tumor growth, while stochastic perturbations introduce variability that mirrors clinical uncertainty. Notably, lower α values indicative of strong memory are associated with delayed immune activation and prolonged tumor survival, whereas higher values approach classical dynamics with enhanced therapeutic efficacy.

The proposed hybrid numerical scheme, combining Caputo–Fabrizio discretization and the Euler–Maruyama method, successfully resolves both deterministic and stochastic regimes with high fidelity. Sensitivity analysis underscores the dominant influence of α on drug dynamics, affirming the critical role of fractional memory in treatment modeling. Spatial and 3D simulations reveal the heterogeneous distribution of biological agents, reinforcing the necessity of spatially explicit modeling in cancer research.

This work advances the frontier of mathematical oncology by demonstrating the importance of incorporating memory and randomness into tumor modeling. The framework offers a powerful tool for optimizing treatment strategies and provides a foundation for future research in personalized medicine, immune modulation, and multi-scale cancer therapy design.

References

[1] Caputo, M., & Fabrizio, M. (2015). A new definition of fractional derivative without singular kernel. Progress in Fractional Differentiation and Applications, 1(2), 73–85. DOI: 10.18576/pfda/010201

[2] Milstein, G. N., and Tretyakov, M. V. (2004). Stochastic Numerics for Mathematical Physics Springer, ISBN: 978-3-540-20945-5

[3] Ansarizadeh, F.; Singh, M.; Richards, D. (2017). Modelling of tumor cells regression in response to chemotherapeutic treatment. Appl. Math. Model. 48, 96–112.

[4] Al-Mekhlafi, S. M. (2025). A novel crossover variable order (deterministic -stochastic) Lung cancer and tumor-immune system interaction: Numerical simulations, Progress in Fractional Differentiation and Applications, 11(1),73-86.

[5] Sweilam, N.H., Al-Mekhlafi, S.M., Ahmed, A., Alsheri, A., Abou-Eldahab, E. (2024). Numerical Treatments for Crossover Cancer Model of Hybrid Variable-Order Fractional Derivatives, 140(2), 1619-1645, https://doi.org/10.32604/cmes.2024.047896.

[6] Sancho-Araiz, A., et al. (2021). The Role of Mathematical Models in Immuno-Oncology: Challenges and Future Perspectives. Pharmaceutics, 13(7).

[7] Butner, J. D., et al. (2022). Mathematical modeling of cancer immunotherapy for personalized clinical translation. Nature Computational Science, 2(12), 785–796.

[8] Bekker, R. A., et al. (2022). Mathematical modeling of radiotherapy and its impact on tumor interactions with the immune system. Neoplasia, 28, 100796.

[9] Dokuyucu, M. A., et al. (2018). Cancer treatment model with the Caputo–Fabrizio fractional derivative. European Physical Journal Plus, 133, 92.

[10] Taba, M. T. (2013). The fractional Fourier transform and its application to digital watermarking. 8th International Workshop on Systems, Signal Processing and their Applications, 262–266.

[11] Lokenath, D. (2003). Recent applications of fractional calculus to science and engineering. International Journal of Mathematics

and Mathematical Sciences, 54, 3413–3442.

[12] Ibrahim, S. N., Misiran, M., & Laham, M. F. (2021). Geometric fractional Brownian motion model for commodity market simulation. Alexandria Engineering Journal, 60, 955–962.

[13] Arfan, M., et al. (2021). On Fractional Order Model of Tumor Dynamics with Drug Interventions under Nonlocal Fractional Derivative. Results in Physics, 21, 103783.

[14] Laksaci1, N., Boudaoui1, A., Al-Mekhlafi, S. M., and Atangana, A. (2023), Mathematical analysis and numerical simulation for fractal-fractional cancer model, Mathematical Biosciences and Engineering, 20(10), 18083–18103, http://www.aimspress.com/journal/mbe 56-

[15] Alinei-Poiana, T., Dulf, E. H., & Kovacs, L. (2023). Fractional calculus in mathematical oncology. Scientific Reports, 13, 10083.

[16] Abou Hasan, M. M., Al-Mekhlafi, S. M. Rihan, F. A., Al-Ali, H. A. (2025). Modeling Hybrid Crossover Dynamics of Immuno-Chemotherapy and Gene Therapy: A Numerical Approach, MMA, 48(8), 8925-8938.

[17] Sweilam, N. H., Al-Mekhlafi,S. M., Abdel Kareem, W.S., Alqurishi, G. (2024). Comparative Study of Crossover Mathematical Model of Breast Cancer Based on Ψ-Caputo Derivative and Mittag-Leffler Laws: Numerical Treatments, Symmetry, 16(9), 1172.

[18] D'Onofrio, A., & Gandolfi, A. (2010). Stochastic models for tumor growth and applications to cancer therapy. Mathematical Biosciences, 228(2), 175-182.

[19] Sarkar, R. R., & Banerjee, S. (2005). Cancer self-remission and tumor stability: a stochastic approach. Mathematical Biosciences, 196(1), 65-81.

[20] Yang, J., & Wang, X. (2015). Stochastic modeling of tumor growth with random noise. Journal of Theoretical Biology, 374, 61-70.

[21] Mainardi, F. (2007). Gorenflo, R., Fractional calculus and stochastic processes. Fractals, 15(3), 251-260.

[22] Kegl, B., Hribernik, A. (2018). Experimental analysis of injection timing and injection pressure impact on emission characteristics of a diesel engine, Applied Energy, 219, 614–627.